Basis-Set Choice for DFT/NEGF Simulations of Carbon Nanotubes

G.B. Abadir · K. Walus · D.L. Pulfrey

Abstract We investigate the effect of the choice of the basis set on the results of *ab initio* (density functional theory/non-equilibrium Green's function) calculations of the bandgap of semiconducting carbon nanotubes, and near-zero-bias conductance of metallic carbon nanotubes. Both ideal and deformed carbon nanotubes are studied, as well as nanotubes with an adsorbed biomolecule. The results show that the near-zero-bias conductance of armchair nanotubes can be calculated accurately with a minimal basis set, with the exception of the (2,2) tube, where a polarized basis set is necessary to accurately predict the metallic behaviour of this tube. For zigzag tubes, a double-zeta polarized basis set is in general required for accuracy in bandgap and near-zero-bias conductance calculations.

Keywords Carbon Nanotubes · DFT · NEGF · Basis Sets

1 Introduction

Carbon nanotubes have been the subject of *ab initio* simulations to investigate a variety of their properties [1,2,3]. It has been suggested already that non-*ab initio* models do not provide accurate results for small-radius nanotubes (*e.g.*, [1, 4]). However, no assessment of the optimal choice of the basis set in *ab initio* simulations has been presented until now. In fact, the improper choice of the basis set can lead to erroneous results, as we demonstrated in an earlier work [1].

G.B. Abadir · K. Walus · D.L. Pulfrey
The Department of Electrical and Computer Engineering
The University of British Columbia
2332 Main Mall, V6T1Z4, Vancouver, BC, Canada
E-mail: georgea@ece.ubc.ca

[1] Abadir, G.B., Walus, K., and Pulfrey, D.L.: Comment on "Curvature effects on electronic properties of small radius nanotube"[Appl. Phys. Lett. 91, 033102 (2007)], Submitted to Appl. Phys. Lett., 15th of September 2008.

In this paper we discuss the effect of the basis set on the results of *ab initio* calculations of the bandgap and near-zero-bias conductance of carbon nanotubes. The near-zero-bias conductance is used to assess the accuracy of the basis sets for the simulation of metallic nanotubes which have a zero-bandgap; and the bandgap is used to assess the accuracy of the basis sets for semiconducting tubes which have a very small near-zero-bias conductance ($\sim$ pS - nS). We first study several ideal nanotubes with different chiralities. We then study the effect of small displacements in the atomic positions on the choice of the basis set. Finally, we study the effect of the addition of an adsorbed biomolecule on the choice of the basis set. The simulations were performed using the density functional theory/non-equilibrium Green's function (DFT/NEGF) approach, within the local density approximation (LDA) [5], employing the Atomistix [6] package described in [7].

2 Simulated Structures

The simulations are divided into three different sets. The first set (SET I) is for perfect nanotubes of different chiralities. The second set (SET II) is for a (10,0) tube with the positions of its atoms having been displaced due to immersion in water. The coordinates of the atoms are determined from a molecular dynamics (MD) simulation of the nanotube in water using the package GROMACS [8]. The third set of simulations (SET III) is for a (10,0) nanotube with an adsorbed dimer of the aromatic amino acid tyrosine, with the coordinates of the tube and tyrosine also determined from MD simulations in water.

For SET I, the simulated structures consisted of a central region of four periods (eight layers of atoms) of each of the armchair tubes: (2,2), (3,3), (4,4), and (5,5); and two periods (also eight layers of atoms) of the zigzag tubes: (4,0),

(8,0), (10,0), (11,0), (13,0), (14,0), (16,0), (17,0), (19,0), and (20,0). The central region was sandwiched between two carbon nanotube electrodes of the same chirality as the central region. For the (n,n) armchair tubes the electrodes consisted each of two periods of the tube (0.4926 nm). For the $(n,0)$ zigzag tubes the electrodes consisted of only one period of the tube (0.4266 nm). In DFT/NEGF simulations, the electrodes are assumed to be repeated infinitely in the transport direction, and to have bulk-like properties [7]. The length of the electrodes was thus chosen to be sufficiently long to ensure that there was no interaction between the central region and the repeated images of the electrodes. The simulation box itself is also repeated in the directions transverse to the transport. The transverse dimensions of the different simulation boxes were gradually increased until no significant change in the results was observed. The basis sets used were the single-zeta (SZ), the single-zeta polarized (SZP), the double-zeta (DZ), and the double-zeta polarized (DZP) [9,10]. The results using the DZP basis set were taken as the reference against which all the other results were compared: the DZP is the most complete basis set we used, and, therefore the one that best predicts the ground state of the system [10]. To further ensure the validity of the DZP basis set as a reference, we repeated the simulations for the (2,2), (3,3), (4,4), (5,5), (4,0), (8,0), (10,0) and (11,0) perfect tubes with the double-zeta double-polarized (DZDP) basis set. For the armchair tubes and the (4,0) metallic tube the maximum difference in calculating the near-zero-bias conductance was 0.1% for the (2,2) tube. For the semiconducting zigzag tubes (8,0), (10,0) and (11,0), the difference between the bandgap calculated from the DZP and the DZDP basis sets was only about 1-2 meV (although both valence and conduction band edges shifted in the same direction by a few meV's relative to the Fermi level in all cases). This assures that no further improvement to the accuracy of the results is likely to be achieved for these tubes by using basis sets higher than the DZP set. Larger systems could not be simulated with the DZDP basis set due to memory limitations. For Set II, five periods of a (10,0) tube were sandwiched between two nanotube electrodes, each consisting of one period of the tube. The coordinates of the central region were calculated from a 2 ns MD simulation of the central region immersed in water. The basis sets used in the subsequent DFT/NEGF simulations were the same as in SET I. For SET III, again five periods of a (10,0) tube were sandwiched between two nanotube electrodes, each consisting of one period of the tube, with the addition of a dimer of the amino acid tyrosine adsorbed on the surface of the central region to simulate the effect of an analyte in a carbon-nanotube-sensor application. The coordinates of the atoms of the central region and the atoms of the dimer were taken from an MD simulation of duration 2 ns. The length of the central region was increased compared to SET I in order to accommodate the adsorbed

molecule. The length in SET II was chosen to be equal to that in SET III to allow for meaningful comparisons.

3 Results and discussion

3.1 SET I

The energy-dependent transmission coefficient $T(E)$ of the (2,2) tube is shown in Fig. 1 for the different basis sets used. $T(E)$ gives the fraction of the electron wave which is transmitted from one electrode to the other [7]. The zero-reference of energy is the Fermi level. The SZ basis set predicts a semiconducting tube with an energy gap of 0.68 eV, the DZ basis set predicts an energy gap of 0.1 eV, while both the SZP and the DZP basis sets give almost identical results, clearly showing a metallic behaviour of the same tube. This result demonstrates that the inclusion of polarization for such a small-diameter tube (0.2716 nm) is essential to get acceptable results. This stems from the fact that polarization models the mixing of different orbitals such as p and d orbitals in carbon [10], a mixing which becomes more apparent as the tube diameter gets smaller. Fig. 2 shows contour plots for the first transmission eigenstate at an energy of 0.05 eV above the Fermi level of the (2,2) tube, as calculated using both the DZ and the DZP basis sets on a plane passing through the tube axis with its normal in the $x-$ direction (with the transport direction being the $z-$ direction). It is clear that the magnitude and shape of the eigenstate is different for the DZP and DZ cases, indicating a significant influence of the mixing of d orbitals with the p orbitals.

In addition to the mixing of p and d orbitals, it is also worth noting that Fig. 2 shows that the transmission eigenstate of the (2,2) tube is asymmetric around the carbon atoms: it consists of one lobe pointing to the exterior of the tube, in addition to a smaller lobe pointing to the interior of the tube. In other words, the transmission eigenstate of the (2,2) tube shows a strong 'blend' of σ orbitals. This is in contrast with the transmission purely due to the π orbitals predicted by the tight-binding models, and which applies for tubes with a diameter larger than 0.7 nm [11]. This suggests that in addition to the $p-$ and $d-$orbitals mixing, a hybridization between the σ and π orbitals also occurs in the (2,2) tube.

The calculated transmission coefficients for the (3,3), (4,4), (5,5), (4,0), (8,0), (10,0), (11,0), (13,0), and the (14,0) tubes are shown in Fig. 3 through Fig. 11. The results for the (16,0), (17,0), (19,0), and the (20,0) tubes are summarized in Fig. 12 and Fig. 13 alongside the other semiconducting zigzag tubes.

For the (3,3) tube, the DZ basis set shows a small dip in $T(E)$ at the Fermi level that is not evident with the other basis sets. Though the SZ basis set gives a result closer to the polarized sets than the DZ set, it poorly predicts the transmission coefficient at higher energies, which, for low

bias levels should not contribute to the current. The near-zero-bias conductance G is calculated according to the equation [12]:

$$G = \frac{2q^2}{h} \int_\mu^\infty (-\frac{\partial f}{\partial E}) T(E) dE \qquad (1)$$

where q is the electronic charge, μ is the Fermi level of the contact with the higher potential, f is the Fermi-Dirac distribution function, and E is the energy. For near zero-bias calculations, μ is taken to be zero, and $T(E)$ is assumed not to vary considerably from the calculations at equilibrium. The values of G are shown in Table 1.

Table 1 near-zero-bias conductance for the metallic tubes in units of S. The subscript of G designates the corresponding tube.

	$G_{(2,2)}$	$G_{(3,3)}$	$G_{(4,4)}$	$G_{(5,5)}$	$G_{(4,0)}$
SZ	3.00e-8	7.73e-5	7.76e-5	7.76e-5	1.16e-4
SZP	1.49e-4	7.75e-5	7.76e-5	7.71e-5	9.32e-5
DZ	2.31e-5	7.62e-5	7.76e-5	7.76e-5	1.35e-4
DZP	1.49e-4	7.75e-5	7.76e-5	7.76e-5	1.05e-4

It can be seen from Table 1 that for the armchair tubes, with the exception of the (2,2) tube, all the basis sets give almost identical values of G. From the corresponding transmission coefficient figures, we can see that all the basis sets predict a metallic (zero-gap) tube except for the (2,2) tube. For the (2,2) tube, the SZP and DZP give the same value of G which is much higher than those predicted from the SZ and DZ calculations. This suggests that the use of even a minimal SZ basis can be adequate for the simulations of armchair tubes with the exception of the (2,2) tube. Table 2 shows the computational resources required for the simulations of the (4,4) tube (160 atoms).

Table 2 Computational resources for both the DZ and DZP basis sets used for computing the data in Fig. 4. Parallel calculations were conducted on a 64-bit, 8-processor (Intel(R) Xeon(TM) 2.66 GHz CPU each) Dell machine.

	Total Memory (GB)	CPU time (h)	Output file size (MB)
SZ	2.0	0.46	4.3
SZP	2.7	1.8	18.4
DZ	2.6	1.48	14.7
DZP	4.0	4.9	37.5

It can be seen that the DZP requires considerably longer time, more memory size, and a much larger amount of disk storage than the other basis sets. These requirements can be very problematic, and even prohibitive, for longer, and/or larger-diameter armchair tubes.

For the (4,0) tube, the value of $T(E)$ at and near the Fermi level with the non-polarized basis sets is significantly different from its value with the polarized ones. For example, at the Fermi level, $T(E)$ is equal to 5 with the DZ basis set, compared to 3 with the polarized basis sets. The same problem occurs with the SZ basis set at an energy just 20 meV below the Fermi level. Since the conduction in such a metallic tube is due to the electrons with energies within a few kT's of the Fermi level (where kT is the thermal energy), this difference in the value of the transmission coefficient is not acceptable, and the inclusion of polarization in the basis set is necessary. Even the SZP basis set predicts a near-zero-bias conductance that is about 11% less than that calculated from the DZP basis set. Therefore, a minimum of a DZP basis set is required to accurately describe the near-zero-bias conductance of the (4,0) tube.

It has to be noted that the metallic behaviour exhibited by the (4,0) tube is in contradiction to the semiconducting behaviour predicted by simple tight-binding models. This is due to the hybridization of the σ and π orbitals (which was also observed for the (2,2) tube as discussed above). This hybridization becomes significant in small-radius tubes [11], and can lead to the observed metallic behaviour of the (4,0) tube [13]. It is important to emphasize that this hybridization is not the same as the mixing of the p and d orbitals mentioned above since the σ and π orbitals arise from the hybridization of the s and p orbitals in carbon. In general, tight-binding $\pi-$bond models have been previously shown to fail for tubes with a diameter smaller than that of the (10,0) tube [1,11].

The $T(E)$ of the (8,0) tube shows an energy gap indicating a semiconducting tube. The SZP overestimates the bandgap by 31 meV compared to the bandgap predicted by the DZP basis set. The DZ and SZ basis sets give values for the gap of 786 meV and 987 meV compared to the 543 meV calculated by the DZP set. The results again suggest the necessity of using the DZP basis set, and the importance of the mixing of p and d orbitals in this tube.

For the semiconducting zigzag tubes larger than the (8,0) tube, the calculated bandgap is shown in Fig. 12. The corresponding difference in the calculcated bandgap (ΔE_G) with respect to that calculated from the DZP basis set (E_{GDZP}) is shown in Fig. 13. This difference depends on the exact chirality of the tube and not only on its diameter. For tubes with $n = 3p + 1$ where p is an integer, the DZ basis set overestimates the gap by about 20 meV for all tubes, while the SZ basis set underestimates the gap by about 40 meV for the (10,0) tube and then the difference decreases gradually with increasing the tube diameter to reach ~ 20 meV for the (19,0) tube. We also notice that the rate of decrease of ΔE_G with respect to n decreases with increasing n. The SZP basis set shows a similar behaviour to the SZ basis set, though the difference in the bandgap with respect to E_{GDZP} is systematically larger than the that for the SZ basis set. For tubes with $n = 3p + 2$, the DZ basis set overestimates the gap com-

pared to E_{GDZP} by 51 meV for the (11,0) tube and the difference decreases gradually to reach 26 meV for the (20,0) tube. The SZ basis set, on the other hand, overestimates the gap by about 20 meV for the (11,0) tube and then the difference decreases rapidly to about 2 meV for (17,0) and (20,0) tubes. Again the SZP set shows a similar behaviour to the SZ set and the difference in the bandgap is larger in the case of the SZP basis set. A similar phenomenon has been obersved in [1] when comparing the bandgap calculated using the $\pi-$bond model and using DFT simulations with a minimal basis set. It is noteworthy from the transmission coefficient graphs that, at energies higher than 750 meV, the non-polarized basis sets always deviate considerably from the DZP basis set, and that at such energies the SZP basis set produces results that most closely match those of the DZP basis set. Therefore, if these energies are of a particular interest, the use of a polarized basis set appears necessary.

The carbon nanotube band structure can be obtained from that of graphene according to the zone-folding scheme [11]. Therefore, to explain why the results of the (n,0) tubes depend on whether $n = 3p + 1$ or $n = 3p + 2$ as mentioned above, we simulated the band structure of graphene using the SZ, DZ, SZP, and DZP basis sets. The lowest conduction subband and the top valence subband are shown in Fig. 14. We then calculated the difference between the lowest conduction subband and the top valence subband (ΔE) at different k-points. The difference at the high-symmetry K point was zero as expected. According to the zone folding (ZF) scheme, only certain values of the **K** vector are allowed, as illustrated by the vertical lines in Fig. 14 for the (10,0), (11,0), (19,0), and (20,0) tubes. The bandgap of tubes with $n = 3p + 1$ is obtained from the lines to the right of the K-point, whereas the bandgap of tubes with $n = 3p + 2$ is obtained from the lines to the left of the K-point. We then calculated the bandgap corresponding to the different semiconducting zigzag tubes mentioned above using different basis sets, and applying the ZF scheme. The difference between the bandgap calculated according to the ZF scheme using the SZ, DZ, and SZP basis sets, and that calculated using the DZP basis set ($\Delta E_{G_{ZF}}$) is shown in Fig. 15. It can be seen from Fig. 15 that $\Delta E_{G_{ZF}}$ still exhibits a non-monotonic trend with respect to the chirality index n similar to that shown in Fig. 13, especially for the SZ and SZP sets, though the exact values are different. Thus, we opine that the trend in bandgap differences between the various basis sets has its origin in the zone-folding scheme used to calculate the band structure of nanotubes from that of graphene.

From the results of SET I, we conclude that for bandgap and near-zero-bias conductance calculations of perfect carbon nanotubes, the choice of the basis set depends on the chirality and the diameter of the tube. For zigzag tubes smaller than the (14,0) tube, a DZP basis set is in general necessary for accurate DFT/NEGF simulations. For the (14,0) tube and
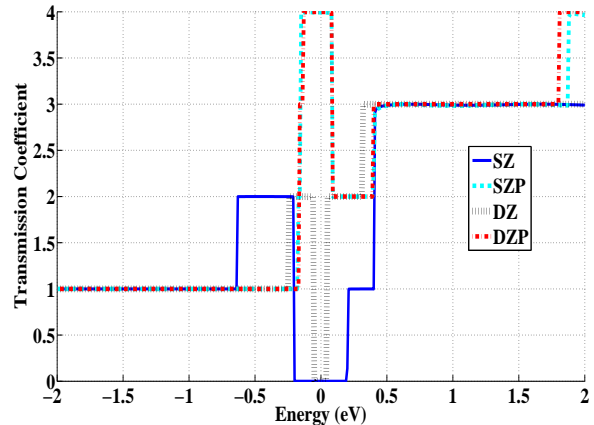
Fig. 1 Transmission coefficient vs. energy for the (2,2) tube with different basis sets.

larger zigzag tubes, if $n = 3p + 1$, a DZP basis set may still be neccessary for DFT/NEGF simulations, whereas if $n = 3p + 2$, the SZ basis set can be sufficient to get an estimation of the bandgap of the tube. For the armchair tubes, a minimal basis set may be sufficient for an accurate estimation of the near-zero-bias conductance, and for a correct qualitative description of the metallic behaviour of these tubes. The exception is the (2,2) tube, which requires a polarized basis set to account for the mixing of p and d orbitals, which appears to play an important role in the properties of the (2,2) tube.

3.2 SET II

The calculated transmission coefficient of a (10,0) tube with atom coordinates determined from an MD simulation of the tube in water is shown in Fig. 16. The maximum displacement of carbon atoms with respect to the ideal case was about 0.3 Å. First, we note that unlike the perfect tubes, the transmission coefficient does not show a step-like behaviour. This is due to the lack of perfect periodicity in the structure, and therefore quantum mechanical reflections may occur at the electrode/central region interface, and within the central region itself.

The calculated bandgap for the DZP, DZ, and SZ basis sets was exactly the same as calculated for the perfect (10,0) tube in SET I. The bandgap calculated by the SZP basis set was 3 meV lower than its counterpart in SET I.

Therefore, we conclude that small displacements in the carbon atom positions need not influence the choice of the basis set, and, in general, a DZP basis set would be recommended for such a simulation unless the system is too large (e.g., a longer tube), in which case memory limitations and/or time requirements may dictate the using of a lower

(a)

(b)
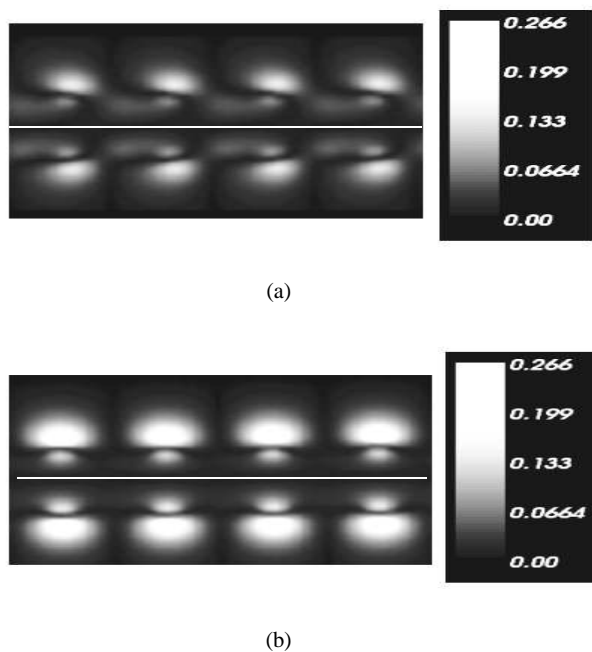
Fig. 2 Zoom-in for the first transmission eigenstate calculated for the (2,2) tube in units of $\text{Å}^{(-3/2)}$ at an energy 0.05 eV above the Fermi level, (a) using the DZ basis set, (b) using the DZP basis set. The horizontal white line in the middle denotes the axis of the tube.
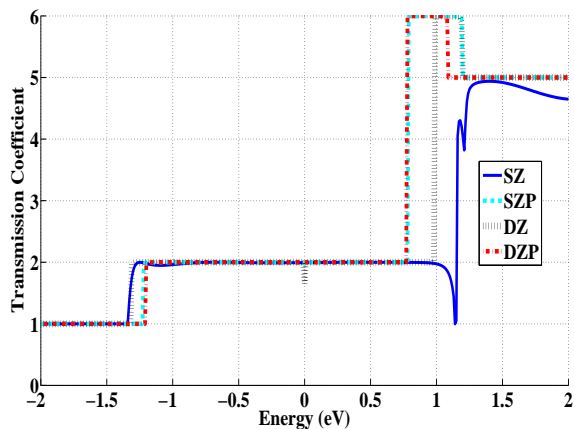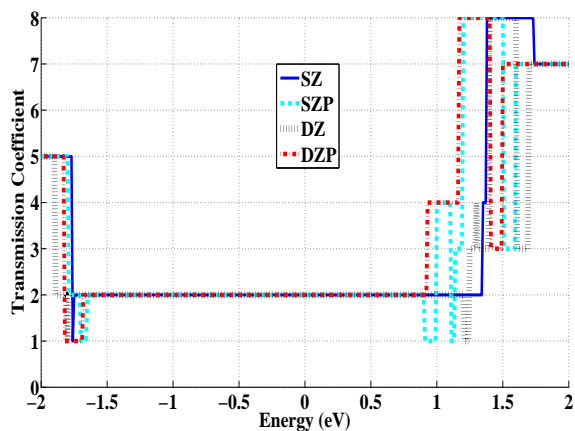

Fig. 3 Transmission coefficient vs. energy for the (3,3) tube with different basis sets.

basis set according to the rules and observations described for SET I.

3.3 SET III

In this set, we investigate the effect of the existence of a physisorbed molecule on the nanotube surface on the choice of the basis set. A 2 ns MD simulation of a (10,0) tube and a dimer of the amino acid tyrosine in water showed that the dimer/nanotube-surface separation was 0.265 nm. We also

Fig. 4 Transmission coefficient vs. energy for the (4,4) tube with different basis sets.
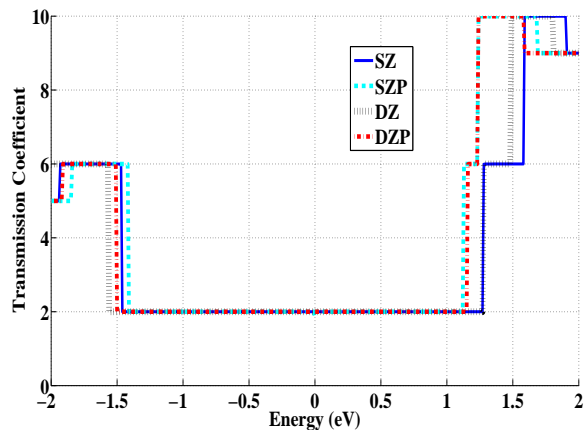
Fig. 5 Transmission coefficient vs. energy for the (5,5) tube with different basis sets.
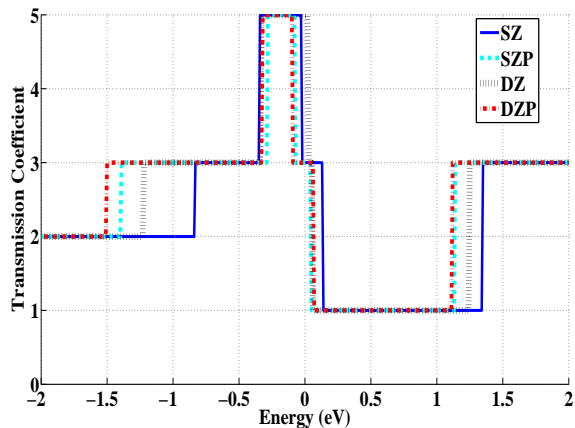
Fig. 6 Transmission coefficient vs. energy for the (4,0) tube with different basis sets.

find that the aromatic rings stack over the hexagonal rings of the nanotube. The configuration at the end of the MD simulation is shown in Fig. 17. The MD simulations are
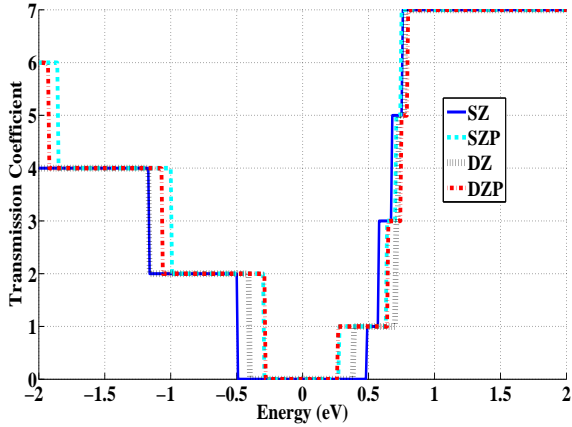
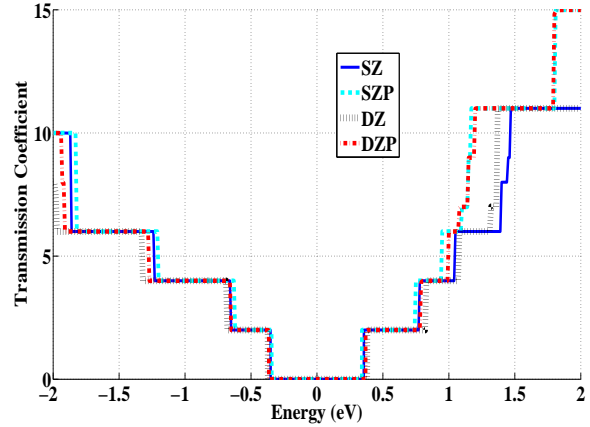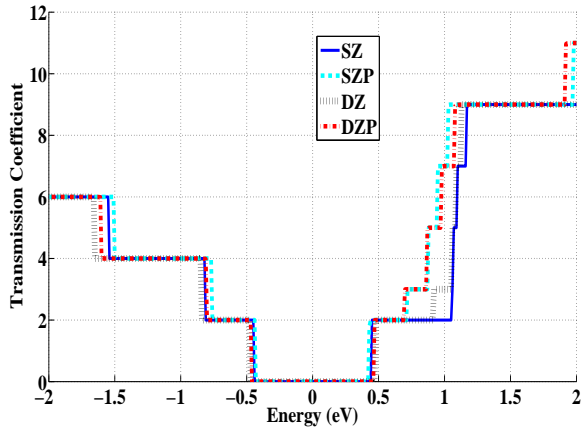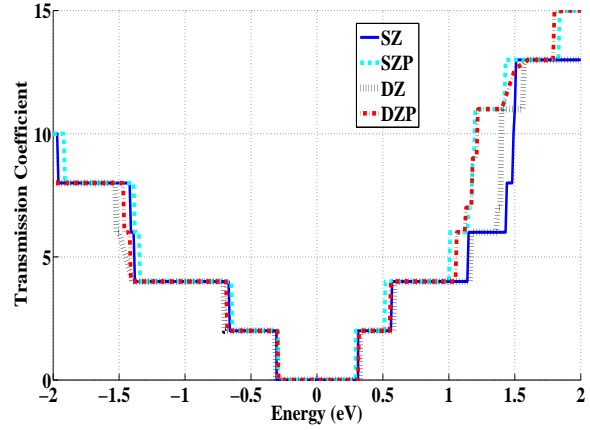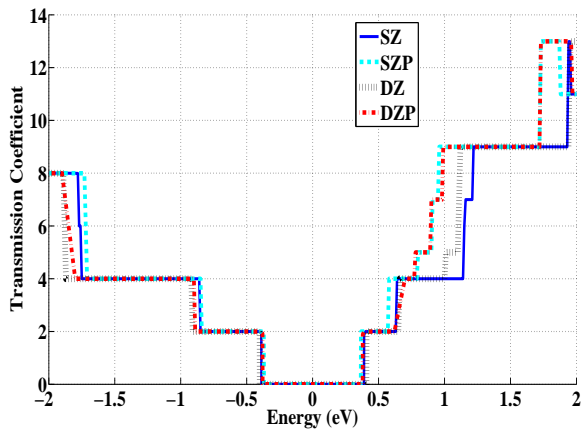**Fig. 7** Transmission coefficient vs. energy for the (8,0) tube with different basis sets.

Fig. 8 Transmission coefficient vs. energy for the (10,0) tube with different basis sets.

Fig. 9 Transmission coefficient vs. energy for the (11,0) tube with different basis sets.
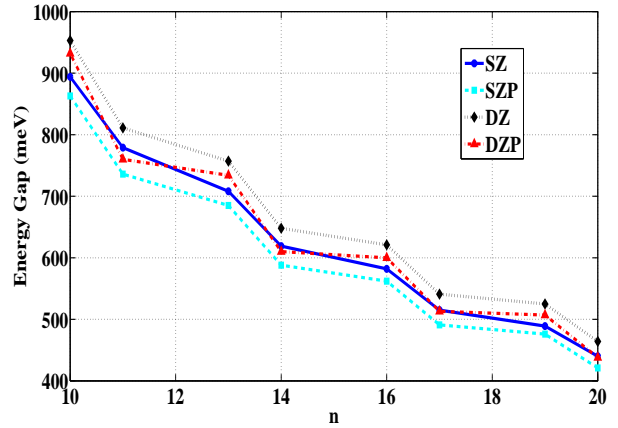

Fig. 10 Transmission coefficient vs. energy for the (13,0) tube with different basis sets.

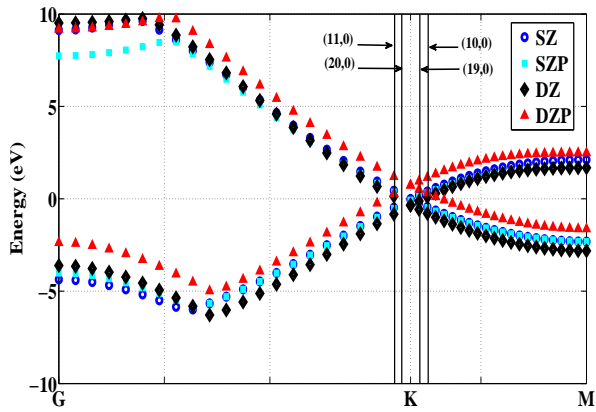**Fig. 11** Transmission coefficient vs. energy for the (14,0) tube with different basis sets.

Fig. 12 Bandgap for the semiconducting (*n*,0) tubes as calculated using different basis sets vs. n.

necessary to get the relative coordinates of the biomolecule and the nanotube since DFT optimization alone does not account for van der Waals forces [14], which are important in

nanotube/biomolecule interactions [15]. The maximum displacement of the atoms of the tube with respect to the ideal case was about 0.3 Å as in SET II. The transmission coeffi-
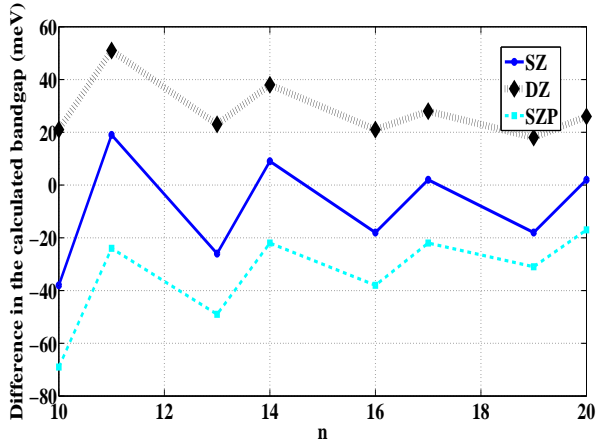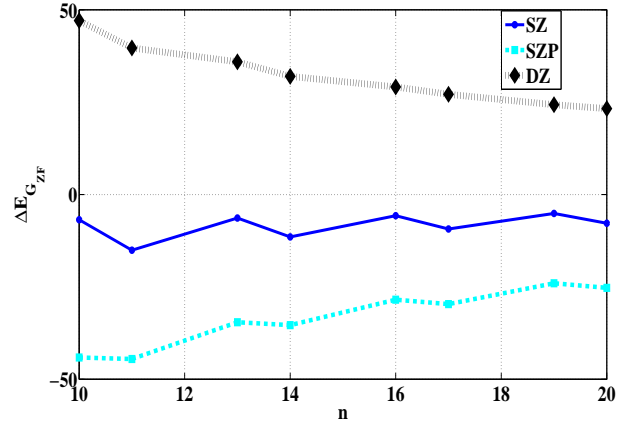
Fig. 13 Difference in the calculated bandgap using the SZ, DZ, and SZP basis sets, and that calculated using the DZP basis set for the semiconducting $(n,0)$ tubes vs. n.

Fig. 15 Difference in the calculated bandgap for the same zigzag tubes shown in Fig. 13 using the SZ, DZ, and SZP basis sets, and that calculated using the DZP basis set, according to the zone-folding scheme.
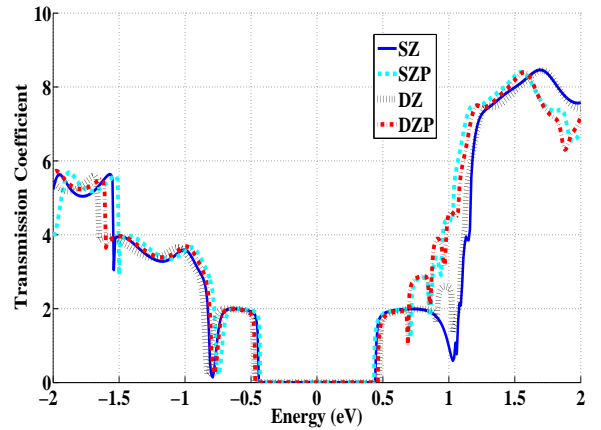

Fig. 14 The lowest conduction subband and the top valence subband of the E-k band diagram of graphene calculated using different basis sets. The G, K, and M points are the high-symmetry points Γ, K, and M, respectively. The vertical lines are the cut-lines at which the bandgap of the (10,0), (11,0), (19,0), and (20,0) tubes is calculated according to the zone-folding scheme. Lines to the left of the K point correspond to $(n,0)$ tubes with $n = 3p + 2$, and lines to the right of the K point correspond to $(n,0)$ tubes with $n = 3p + 1$.

Fig. 16 Transmission coefficient vs. energy for the (10,0) tube after an MD simulation, and with different basis sets.

cient resulting from the subsequent DFT/NEGF simulations is shown in Fig. 18. The results are very similar to those of SET II in the sense that the DZ and DZP sets exhibit a rather good agreement in the range of energies within a few kT's above the edge of the lowest conduction subband (E_C), and that at higher energies the DZ and DZP results deviate from each other. At these energies the SZP is in better agreement with the DZP basis set, indicating a more significant effect of the polarization. The calculated bandgap was 898 meV for the SZ basis set, 867 meV for the SZP basis set, 954 meV for the DZ basis set, and 932 meV for the DZP basis set. Comparing these results with the results shown in Fig. 12, it is clear that the physisorbed biomolecule did not have a significant effect on the calculated bandgap for all ba-

sis sets. However, one important parameter that can be quite sensitive to the basis set is the Mulliken population [16], from which the electron density is calculated. Set III is particularly prone to such a sensitivity due to the presence of an adsorbed molecule and the possible orbital overlap between the nanotube and the biomolecule. The charge transfer between the tube and the biomolecule is an important factor in the nanotube/biomolecule interaction. The charge transferred from the amino acid to the tube was calculated to be $0.3057q$ in the case of the DZP basis set (Q_{DZP}), $0.3306q$ in the case of the DZ basis set (Q_{DZ}), $0.702q$ in the case of the SZP basis set (Q_{SZP}), and $0.8474q$ in the case of the SZ basis set (Q_{SZ}). The difference between Q_{DZ} and Q_{DZP} is only $0.0249q$ compared to $0.3963q$ for the difference between Q_{SZP} and Q_{DZP}, and $0.5417q$ for the difference between Q_{SZ} and Q_{DZP}. The Mulliken population calculated for each carbon atom on the tube showed a maximum difference of less than 1% for the DZ set compared to the DZP

basis set. The SZ and SZP basis sets show higher relative difference compared to the DZ basis set, especially for the dimer atoms. Although the DZ basis set also shows relatively large differences in the Mulliken population for the dimer atoms (especially in hydrogen atoms where we observed a relative difference of around 20%), these differences did not have a significant impact on the total electronic charge of the amino acid, or on the electronic density in the tube, or the transmission coefficient of the tube. In general, a DZP basis set is required for such a simulation, and the SZ or the SZP basis sets would not accurately predict the Mulliken population. The resources required to perform such a simulation using the DZP basis set and the DZ basis set are shown in Table 3. It is clear that the DZP basis set requires a significantly larger amount of time and memory resources, which may not be available. In such a case, a DZ basis set may be adequate for the simulation. Another solution could be to use different basis sets for different atoms, *i.e.*, use a polarized basis set to describe the atoms of the biomolecule and a lower basis set to describe the atoms of the carbon nanotube. However, this should be done very carefully since using different basis sets for different atoms can introduce the so-called 'basis set superposition error' [17].
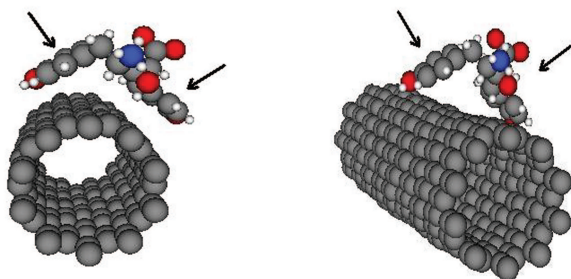
Fig. 17 Different views for the configuration of the central region of the srtucture simulated in Set III following a 2 ns MD simulation. The arrows indicate the aromatic rings of the tyrosine dimer.

Table 3 Computational resources for both the DZ and DZP basis sets used for computing the data in Fig. 18. Parallel calculations were conducted on a 64-bit, 8-processor (Intel(R) Xeon(TM) 2.66 GHz CPU each) Dell machine.

Basis set	Total Memory (GB)	CPU time (h)	Output file size (MB)
DZ	16	132.97	22
DZP	24	259.02	56
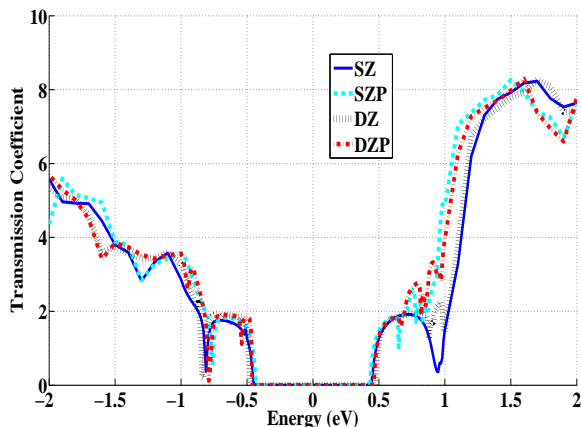
Fig. 18 Transmission coefficient vs. energy for the (10,0) tube with an adsorbed tyrosine dimer after an MD simulation, and with different basis sets.

4 Conclusion

We studied the effect of the basis set choice in *ab initio* DFT/NEGF simulations on the transmission coefficient, near-zero-bias conductance, and bandgap of various carbon nanotubes. The results show that for armchair tubes, a minimal basis set can be sufficient to get an accurate estimation of the near-zero-bias conductance, with the exception of the (2,2) tube, for which polarization should be included to get the near-zero-bias conductance and to capture the metallic behaviour of this tube. For zigzag tubes, we find that the choice of the basis set depends on both the diameter and the chirality of the tube. We found that small displacements in the atomic positions do not affect the choice of the basis set, and that for systems containing both a nanotube and a physisorbed biomolecule, a double-zeta polarized basis set is recommended for an accurate Mulliken population analysis.

Acknowledgements

References

1. Shah, D., Bruque, N.A., Alam, K., Lake, R.K., and Pandey, R.R.: Electronic properties of carbon nanotubes calculated from density functional theory and the empirical $\pi-$bond model, J. Comp. Elec. **6**, 395-400 (2007).
2. Yan, Q., Wu, J., Zhou, G., Duan, W., and Gu, B.: *Ab initio* study of transport properties of multiwalled carbon nanotubes, Phys. Rev. B **72**, 155425 (2005).

3. Sun, P., Kim, H., So, H., Kong, K., Chang, H., Ryu, B., Choi, Y., Lee, J., Kim, B., Kim, J., and Kim, J.: Investigation of the humidity effect on the electrical properties of single-walled carbon nanotube transistors, App. Phys. Lett. **87**, 093101 (2005).

4. Zeng, H., Hu, H.F., Wei, J.W., Wang, Z.Y., Wang, L., and Peng,P.: Curvature effects on electronic properties of small radius nanotube, Appl.Phys. Lett. **91**, 033102 (2007).

5. Perdew, J.P., and Zunger, A.: Self-interaction correction to density-functional approximations for many-electron systems, Phys. Rev. B **23**, 5048-5079 (1981).

6. Atomistix v.2008.02, www.quantumwise.com.

7. Stokbro, K., Taylor, J., Brandbyge, M., and Guo, H.: *Ab-initio* Non-Equilibrium Greens Function Formalism for Calculating Electron Transport in Molecular Devices. In: Cuniberti, G. Fagas, G., and Richter, K. (eds.): Introducing Molecular Electronics (lecture Notes in Physics), 117-152, Springer, Berlin/Heidelberg, (2005).

8. Lindahl, E., Hess, B., and van der Spoel, D.: GROMACS 3.0: A package for molecular simulation and trajectory analysis, J. Mol. Mod. **7**, 306-317 (2001).

9. Koch, W., Holthausen, M.C.: A Chemists Guide to Density Functional Theory, Second edition, 97-101, Wiley-VCH Verlag GmbH (2001).

10. Cramer, C.J.: Essentials of Computational Chemistry: Theories and Models, Second edition, 170-175, John Wiley & Sons Ltd. (2002).

11. Saito, R., Dresselhaus, G., and Dresselhaus, M.S.: Physical Properties of Carbon Nanotubes, 59-72, Imperial College Press (2005)

12. Davies, J.: The Physics of Low-Dimensional Semiconductors: An Introduction, 165, Cambridge University Press (1998).

13. Iyakutti, K., Rajarajeswari, M., and Dharma-wardana, M.W.C.: The interaction of nitrogen molecules with (4, 0) single-walled carbon nanotube: electronic and structural effects, Nanotech. **19**, 185704, (2008).

14. Simeoni, M., Picozzi, S., and Delley, B.: An ab-initio study of pentacene on aluminum (1 0 0) surface, Surf. Sci. **562**, 43-52 (2004).

15. Roman, C., Ciontu, F., Courtois, B.: Aromatic amino acids physisorbed on graphene: electronic properties and Hamiltonian reduction, European Micro and Nano Systems 2004 (EMN04), Paris, France (2004).

16. Sung, D., Hong, S., Kim, Y., Park, N., Kim, S., Maeng, S., and Kim, K.: *Ab initio* study of the effect of water adsorption on the carbon nanotube field-effect transistor, Appl. Phys. Lett. **89**, 243110 (2006).

17. Lewars, E.: Computational Chemistry: Introduction to the Theory and Applications of Molecular and Quantum Mechanics, 251-253, Kluwer Academic Publishers (2003).